

# Synthesis of a Novel Allyl-Functionalized Deep Eutectic Solvent to Promote Dissolution of Cellulose

Hongwei Ren,<sup>a,♀,b</sup> Chunmao Chen,<sup>a,♀</sup> Shaohui Guo,<sup>a</sup> Dishun Zhao,<sup>b</sup> and Qinghong Wang<sup>a,\*</sup>

Deep eutectic solvents (DESs) offer attractive options for the “green” dissolution of cellulose. However, the protic hydroxyl group causes weak dissolving ability of DESs, requiring the substitution of hydroxyl groups in the cation. In this study, a novel allyl-functionalized DES was synthesized and characterized, and its possible effect on improved dissolution of cellulose was investigated. The DES was synthesized by a eutectic mixture of allyl triethyl ammonium chloride ([ATEAm]Cl) and oxalic acid (Oxa) at a molar ratio of 1:1 and a freezing point of 49 °C. The [ATEAm]Cl-Oxa exhibited high polarity (56.40 kcal/mol), dipolarity/polarizability effects (1.10), hydrogen-bond donating acidity (0.41), hydrogen-bond basicity (0.89), and low viscosity (76 cP at 120 °C) owing to the  $\pi$ - $\pi$  conjugative effect induced by the allyl group. The correlation between temperature and viscosity on the [ATEAm]Cl-Oxa fit the Arrhenius equation well. The [ATEAm]Cl-Oxa showed low pseudo activation energy for viscous flow (44.56 kJ/mol). The improved properties of the [ATEAm]Cl-Oxa noticeably promoted the solubility (6.48 wt.%) of cellulose.

*Keywords:* Deep eutectic solvent; Cellulose; Dissolution; Allyl triethyl ammonium chloride

*Contact information:* a: State Key Laboratory of Heavy Oil Processing, China University of Petroleum, Beijing 102249, P. R. China; b: School of Science, Hebei University of Science and Technology, Shijiazhuang 050018, P. R. China; ♀ These authors contributed equally to this work;

\* Corresponding author: wangqhqh@163.com

## INTRODUCTION

Cellulose is the most abundant biopolymer on earth (Klemm *et al.* 2005; Huber *et al.* 2012; Ramamoorthy *et al.* 2015). However, its utilization as an isolated polymer is hindered by its water-insoluble crystalline structure and highly packed polymeric macromolecules (Gümüşkaya *et al.* 2002; Sathitsuksanoh *et al.* 2013). Dissolution, which prepares for the subsequent hydrolysis, saccharification, catalyzed reaction, *etc.*, is the principal step of cellulose processing (Alvira *et al.* 2010; Gericke *et al.* 2012; Chowdhury *et al.* 2014; Castro *et al.* 2015). Conventional solvents, including sulfuric acid, phosphoric acid, lithium chloride/N, N-dimethylacetamide, sodium hydroxide/urea, and tetrabutylammonium fluoride trihydrate/dimethyl sulfoxide, have shown efficient ability to dissolve cellulose (Boerstoel *et al.* 2001; Nayak *et al.* 2008; Ru *et al.* 2015). However, the conventional solvents involved in dissolution processing potentially cause severe environmental pollution (Sun *et al.* 2011). Even the ionic liquids (ILs), which are generally recognized as “green” solvents, have recently been argued against for their poor biodegradability. The environmental concerns require “greener” solvents for the dissolution of cellulose (Pretti *et al.* 2008; Neumann *et al.* 2014).

The deep eutectic solvents (DESs), which are synthesized by a eutectic mixture of a hydrogen-bond acceptor (HBA) and a hydrogen-bond donor (HBD), have recently

emerged as a new class of solvents (Abbott *et al.* 2003). They have been used as various media, such as extractants, electrolytes, catalysts, and solvents. This is due to their advantages of low environmental impact, high reactivity, and low cost (Tang and Row 2013; Paiva *et al.* 2014; Juneidi *et al.* 2015). The choline chloride (ChCl)-based DESs exhibit potential to dissolve various biopolymers, such as refined cork, starch,  $\alpha$ -chitin, and microcrystalline cellulose (Garcia *et al.* 2010; Hou *et al.* 2012; Zhang *et al.* 2012a; Xia *et al.* 2014). However, the solubility for cellulose is usually less than 1.0 wt.% due to the presence of protic hydroxyl ( $-OH$ ) groups in the choline cation (Francisco *et al.* 2012; Itoh 2014; Badgajar and Bhanage 2015). The competition to react with chloride between protic  $-OH$  groups in the choline cation and hydrogen bonds in the cellulose causes decreased solubility. Therefore, the substitution of the protic  $-OH$  groups in the choline cation potentially improves the dissolving ability of ChCl-based DESs. However, the substitution of the  $-OH$  groups by direct etherification is quite difficult due to the relatively inert hydrogen in the choline cation (Vigier and Jérôme 2013). The allylation of the  $-OH$  groups may be an alternative substitution process based on experiences to form allyl-functionalized ILs (Zhang *et al.* 2005; Vitz *et al.* 2009; Ohira *et al.* 2012; Tang and Row 2013; Zhang *et al.* 2015).

The experiments in this study were designed to synthesize a new allyl-functionalized DES to promote the dissolution of cellulose. The solvation properties of allyl-functionalized DES, including Kamlet-Taft polarity model parameters and polarity, were characterized, and the possible effect of improved dissolution of cellulose was investigated.

## EXPERIMENTAL

### Materials

The cellulose used was cotton linter pulp with a polymerization degree of 575.6 (Helon, China). The cotton linter pulp was cut into small pieces and dried at 100 °C for 12 h. The ChCl was recrystallized with ethanol, filtered, and dried under vacuum prior to experimentation (Abbott *et al.* 2004) (Beijing, China). The imidazolium (Im) was dried at 50 °C for 5 h prior to use (Beijing, China). All chemical reagents, including triethylamine, allyl chloride, acetone, and oxalic acid (Oxa), were of analytical grade and purchased from Beijing Chemical Reagents Co. (Beijing, China). The indicators of 2,6-dichloro-4-(2,4,6-triphenyl-1-pyridinio) phenolate (Reichardt's dye 30, RD), 4-nitroaniline (NA), and N,N-diethyl-4-nitroanilin (DNA) were purchased from Fluorochem Ltd. (Old Glossop, UK).

### Synthesis of Allyl-functionalized DES

The target allyl-functionalized DES was synthesized in a two-step process (Fig. 1). The allyl-functionalized ChCl was synthesized first, as previously described (Bergthaller 1980; Du *et al.* 2013; Isik *et al.* 2013).

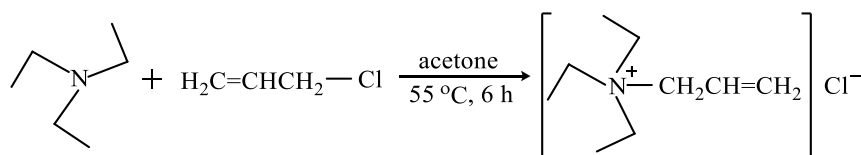


Fig. 1. Synthetic routes of the [ATEAm]Cl-Oxa

Triethylamine and allyl chloride, at a molar ratio of 1:1.10, were added into an acetone solvent in a 250-mL flask integrated with a reflux condenser under nitrogen atmosphere. The mixture was stirred at 55 °C for 6 h. After the acetone solvent was decanted, the solid product was placed at room temperature. The white crystal produced was allyl triethyl ammonium chloride ([ATEAm]Cl).

The allyl-functionalized DES was then synthesized in accordance with previously described methods. The [ATEAm]Cl as a HBA and the Oxa as a HBD were added into a 250-mL flask at different molar ratios. The mixtures were heated and stirred until the homogeneous liquid phase formed. The resultant liquid was dried under vacuum at 60 °C for 24 h to obtain the product of [ATEAm]Cl-Oxa.

The ChCl-Oxa, as a conventional DES with protic –OH groups in the choline cation, was synthesized as described (Abbott *et al.* 2003).

### Analysis of ChCl-DESs

The thermogravimetric properties of the ChCl-DESs were measured by loading a sample into a TG209 TG/DSC thermal analyzer (Netzsch Inc., Selb, Germany). The sample was first cooled to the required temperature, such as -20 °C, and then heated to 140 °C at a rate of 1 °C/min. The freezing temperature was obtained at the temperature when the ChCl-DESs solid began to melt.

Fourier transform infrared spectroscopy (FTIR) and nuclear magnetic resonance (NMR) were used to analyze the structure of the DESs on a FTS-135 Fourier transform infrared spectroscope (Bio-Rad, Hercules, CA, USA) and an AVANCE III NMR spectrometer (Bruker, Karlsruhe, German), respectively. The viscosity was measured by a VS4450 rotational viscometer (Marimex, Bielefeld, Germany).

The polarity scale ( $E_T(30)$ ), dipolarity/polarizability effects ( $\pi^*$ ), hydrogen-bond donating acidity ( $\alpha$ ), and hydrogen-bond basicity ( $\beta$ ) were calculated by Eqs. 1 through 6, according to Kamlet-Taft empirical polarity scales (Kamlet and Taft 1976; Taft and Kamlet 1976),

$$E_T(30) = 28592 / \lambda_{\max(RD)} \quad (1)$$

$$\alpha = 0.0649E_T(30) - 2.03 - (0.72\pi^*) \quad (2)$$

$$\pi^* = 0.649 - 0.314\nu_{(NA)} \quad (3)$$

$$\beta = (1.035\nu_{(DENA)} + 2.64 - \nu_{(NA)}) / 2.80 \quad (4)$$

where,

$$\nu_{(NA)} = 1 / (\lambda_{\max(NA)} \times 10^{-4}) \quad (5)$$

$$\nu_{(DENA)} = 1 / (\lambda_{\max(DENA)} \times 10^{-4}) \quad (6)$$

Here,  $\lambda_{\max}$  represents the wavelength of maximum absorption.

### Dissolution of Cellulose

Cellulose was gradually added into 10 g of allyl-functionalized DES in a flask under nitrogen protection. The dissolution of cellulose was investigated within a temperature range of 60 °C to 120 °C, with intervals of 10 °C. The dissolution was monitored with a polarization microscope. When the solution mixture became optically transparent under the polarization microscope, additional cellulose was added until cellulose could not be dissolved further within 2 h, which meant the dissolution of cellulose was completed. Ethyl alcohol was added into the cellulosic solution. After the solution was filtered with a

Büchner funnel and washed by deionized water, the regenerated cellulose was obtained. The regenerated cellulose was dried at 80 °C for 24 h prior to characterization.

### Analysis of Cellulose

The dissolving process was observed with a XP-203 polarization microscope (PLM) (Changfang, Shanghai, China). The structure was analyzed according to a previously created FTIR method. The crystal form was judged by an XRD-6000 X-ray powder diffraction (XRD) (Shimadzu, Tokyo, Japan) with 40.0 kV and a 40.0 mA electric current in the cube target X-ray tube. The surface morphology was observed on an S-4800 scanning electron microscope (SEM) (Hitachi, Tokyo, Japan). The solubility of cellulose was calculated in terms of mass of cellulose dissolved per g DESs (g/g).

The crystallinity index (*CrI*) was calculated from the diffracted intensity results using the empirical method (Segal *et al.* 1959; Saelee *et al.* 2016),

$$CrI (\%) = (I_{002} - I_{am}) \times 100 / I_{002} \quad (7)$$

where *CrI* represents the degree of crystallinity and  $I_{002}$  is the maximum intensity of the principal peak (002) lattice diffraction. For cellulose I,  $2\theta$  is 22.6° and for cellulose II,  $2\theta$  is 20.8°.  $I_{am}$  is the diffraction intensity of amorphous cellulose between the plane (200) and (110). For cellulose I,  $2\theta$  is 18.0° and for cellulose II,  $2\theta$  is 16.0°.

## RESULTS AND DISCUSSION

### Synthesis of Allyl-functionalized DES

The molar ratios of HBA to HBD were closely related to the successful synthesis of a DES (Abbott *et al.* 2003; 2004). The lowest freezing point ( $T_f$ ) of the eutectic mixture occurred at a molar ratio of [ATEAm]Cl to Oxa at 1:1 (Fig. 2). The  $T_f$  value of the eutectic mixture was close to that of ChCl-Oxa (34 °C), but far lower than that of [ATEAm]Cl (368 °C) and Oxa (189 °C). The low  $T_f$  value suggested the interaction happened between [ATEAm]Cl and Oxa, and the [ATEAm]Cl-Oxa DES synthesized.

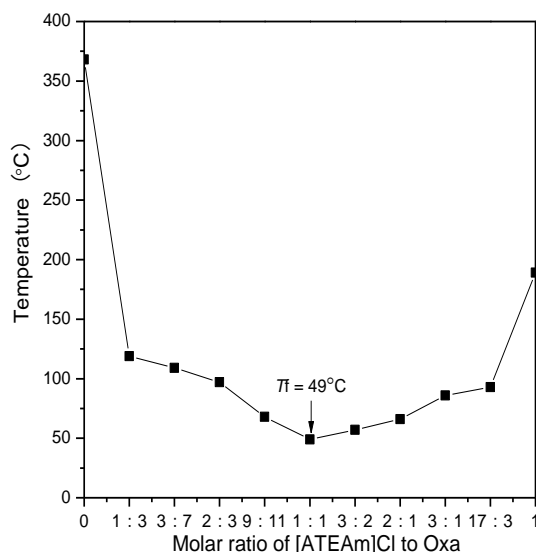


**Fig. 2.** The freezing point ( $T_f$ ) values of eutectic mixture at different molar ratios of [ATEAm]Cl to Oxa

## Structure of ChCl-DESS

The structure of [ATEAm]Cl and [ATEAm]Cl-Oxa was further analyzed. An allyl-functionalized DES, the [ATEAm]Cl-Oxa, was successfully synthesized according to the FTIR and NMR results.

The characteristic peaks of [ATEAm]Cl based on FTIR (KBr) were  $2987\text{ cm}^{-1}$  ( $\nu_{\text{asCH}}$ ,  $\text{CH}_2$ , m),  $1642\text{ cm}^{-1}$  ( $\nu_{\text{SCH}}$ ,  $\text{C}=\text{C}$ , m),  $1484\text{ cm}^{-1}$  ( $\delta_{\text{CH}}$ ,  $\text{CH}_3$ , s),  $1365\text{ cm}^{-1}$  ( $\nu_{\text{CH}}$ ,  $\text{C}=\text{C}$ , w),  $1164\text{ cm}^{-1}$  ( $\delta_{\text{c-c}}$ ,  $\text{C}-\text{C}$ , w),  $1010\text{ cm}^{-1}$  ( $\nu_{\text{SC-H}}$ ,  $\text{C}-\text{C}$ , m),  $958\text{ cm}^{-1}$  ( $\nu_{\text{asC-H}}$ ,  $\text{RCH}=\text{CHR}'$ , w),  $796\text{ cm}^{-1}$  ( $\nu_{\text{SC-H}}$ ,  $\text{C}-\text{C}$ , s), and  $688\text{ cm}^{-1}$  ( $\nu_{\text{SCH}}$ ,  $\text{RCH}=\text{CHR}'$ , w). The hydrogen shifts of [ATEAm]Cl based on  $^1\text{H}$  NMR (500 MHz,  $\text{CDCl}_3$ ) were 5.593 ppm (1H, s,  $\text{N}=\text{CH}-\text{C}$ ), 4.132~4.120 ppm (2H, d,  $\text{N}-\text{CH}_2-\text{C}=\text{C}$ ), 3.506~3.464 ppm (6H, m,  $\text{N}(\text{CH}_2\text{C})_3$ ), 2.345 ppm (2H, s,  $\text{N}-\text{C}-\text{C}=\text{CH}_2$ ), and 1.445~1.405 ppm (9H, m,  $\text{N}(\text{CCH}_3)_3$ ). The characteristic peaks of [ATEAm]Cl-Oxa based on FTIR (KBr) were  $3399\text{ cm}^{-1}$  ( $\nu_{\text{SOH}}$ ,  $\text{COOH}$ , s),  $2985\text{ cm}^{-1}$  ( $\nu_{\text{asCH}}$ ,  $\text{CH}_2$ , m),  $1641\text{ cm}^{-1}$  ( $\nu_{\text{SCH}}$ ,  $\text{C}=\text{C}$ , m),  $1480\text{ cm}^{-1}$  ( $\delta_{\text{CH}}$ ,  $\text{CH}_3$ , s),  $1395\text{ cm}^{-1}$  ( $\nu_{\text{CH}}$ ,  $\text{C}=\text{C}$ , w),  $1189\text{ cm}^{-1}$  ( $\delta_{\text{c-c}}$ ,  $\text{C}-\text{C}$ , w),  $1012\text{ cm}^{-1}$  ( $\nu_{\text{SC-H}}$ ,  $\text{C}-\text{C}$ , m),  $958\text{ cm}^{-1}$  ( $\nu_{\text{asC-H}}$ ,  $\text{RCH}=\text{CHR}'$ , w),  $796\text{ cm}^{-1}$  ( $\nu_{\text{SC-H}}$ ,  $\text{C}-\text{C}$ , s), and  $682\text{ cm}^{-1}$  ( $\nu_{\text{SCH}}$ ,  $\text{RCH}=\text{CHR}'$ , w). The hydrogen shifts of [ATEAm]Cl-Oxa based on  $^1\text{H}$  NMR (500 MHz,  $\text{CDCl}_3$ ) were 7.263 ppm (2H, s,  $\text{HOOC}-\text{COOH}$ ), 5.81 ppm (1H, s,  $\text{N}=\text{CH}-\text{C}$ ), 4.143~4.128 ppm (2H, d,  $\text{N}-\text{CH}_2-\text{C}=\text{C}$ ), 3.511~3.467 ppm (6H, m,  $\text{N}(\text{CH}_2\text{C})_3$ ), 2.111 ppm (2H, s,  $\text{N}-\text{C}-\text{C}=\text{CH}_2$ ), and 1.449~1.419 ppm (9H, m,  $\text{N}(\text{CCH}_3)_3$ ). The carbon shifts of [ATEAm]Cl-Oxa based on  $^{13}\text{C}$  NMR (500 MHz, DMSO) were 161.73~161.71 ppm ( $\text{HOOC}-\text{COOH}$ ), 127.24 ppm ( $\text{NC}-\text{C}=\text{C}$ ), 126.17 ppm ( $\text{NC}-\text{C}=\text{C}$ ), 52.62 ppm ( $\text{NC}-\text{C}=\text{C}$ ), 40.32~39.66 ppm ( $(\text{CH}_2)_3$ ), and 7.68 ppm ( $(\text{CH}_3)_3$ ). The newly appeared chemical peaks ( $3399\text{ cm}^{-1}$ ) in FTIR spectra, 7.263 ppm (2H, s,  $\text{HOOC}-\text{COOH}$ ), and high-fields moves in  $^1\text{HNMR}$  spectra demonstrated that [ATEAm]Cl and Oxa were interconnected through hydrogen bonds.

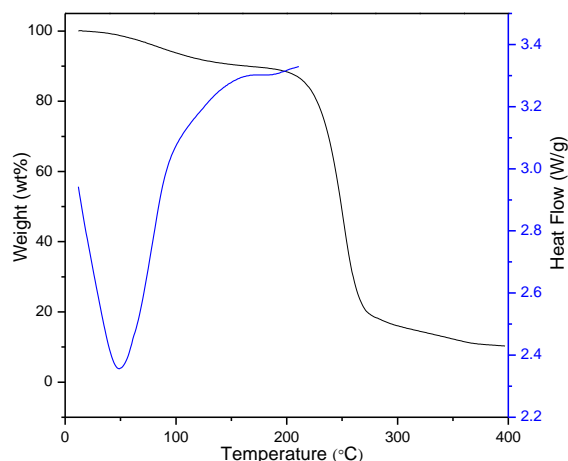


Fig. 3. TGA (in nitrogen) curves of the [ATEAm]Cl-Oxa

## Properties of Allyl-functionalized DES

### Thermostability of ChCl-DESS

The temperatures of 163 °C and 258 °C coincided with weight losses of 10% and 90%, respectively, in [ATEAm]Cl-Oxa, according to thermogravimetric analysis (TGA) (Fig. 3). The results indicated that [ATEAm]Cl-Oxa was steady up to 163 °C. The dissolution temperature of cellulose was usually below 120 °C to prevent carbonation (Kilpeläinen *et al.* 2007; Wang *et al.* 2012). Therefore, the [ATEAm]Cl-Oxa showed sufficient thermostability for the dissolution of cellulose.

### Solvation properties

The Kamlet-Taft polarity model has been widely employed to evaluate the solvation properties of solvents (Badgular and Bhanage 2015). Polarity ( $E_T(30)$ ) and three solvent parameters,  $\pi^*$ ,  $\alpha$ , and  $\beta$ , were employed to investigate the solvation properties of [ATEAm]Cl-Oxa, based on the Kamlet-Taft polarity model (Abbott *et al.* 2003; Spange *et al.* 2003; Taft *et al.* 2003). The parameters of [ATEAm]Cl-Oxa and ChCl-Oxa are listed in Table 1. The  $E_T(30)$ ,  $\pi^*$ ,  $\alpha$ , and  $\beta$  values of [ATEAm]Cl-Oxa were all higher than those of ChCl-Oxa. The allyl group induced the  $\pi$ - $\pi$  conjugative effect on [ATEAm]Cl-Oxa (Badgular and Bhanage 2015; Zhao *et al.* 2012). The charge was delocalized between the allyl group and the choline cation. The enhanced charge mobility in [ATEAm]Cl-Oxa resulted in higher solvent than ChCl-Oxa. The enhanced solvation properties *via* allylic substitution improved the dissolving ability of [ATEAm]Cl-Oxa.

**Table 1.** Solvation Properties of the [ATEAm]Cl-Oxa and ChCl-Oxa (25 °C)

Solvents	$E_T(30)$ kcal mol <sup>-1</sup>	$\pi^*$	$\alpha$	$\beta$
[ATEAm]Cl-Oxa	56.40	1.10	0.41	0.89
ChCl-Oxa	47.78	0.92	0.24	0.52

### Viscosity

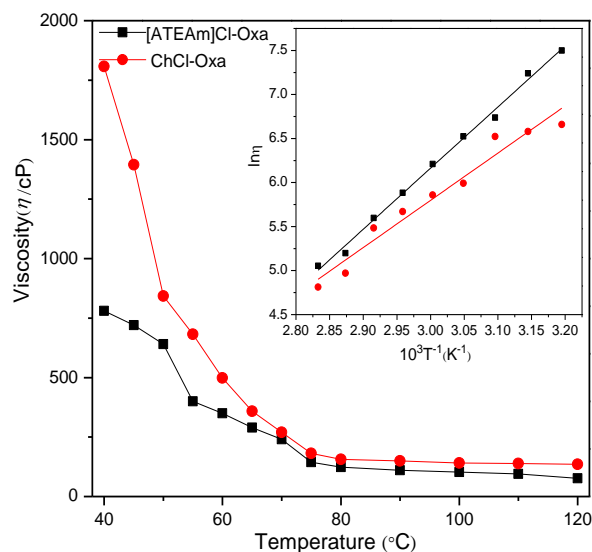
The solubility of cellulose was dynamically dependent on the viscosity of the solvents (Cruz *et al.* 2012; Francisco *et al.* 2013; Badgular and Bhanage 2015). Low viscosity benefited the accessibility of the solvent with hydrogen bonds in cellulose. Most of the DESs exhibited high viscosity, limiting their dissolving ability (Tang and Row 2013; Paiva *et al.* 2014). The low viscosity of the allyl-functionalized DESs was expected based on previous reports on allyl-functionalized ILs. The viscosity of the two DESs decreased as temperature increased (Fig. 4). The [ATEAm]Cl-Oxa showed far lower viscosity than ChCl-Oxa at the same temperature. The viscosity of [ATEAm]Cl-Oxa decreased from 780 cP to 76 cP as temperature increased from 40 °C to 120 °C. The low viscosity was most likely caused by the charge delocalization between the allyl group and the ammonium cation (Zavrel *et al.* 2009). The viscosity-temperature relationship of the two DESs fits the Arrhenius equation (Eq. 8) well (Zhang *et al.* 2012b; Badgular and Bhanage 2015),

$$\ln \eta = \ln \eta_0 + E_\eta / RT \quad (8)$$

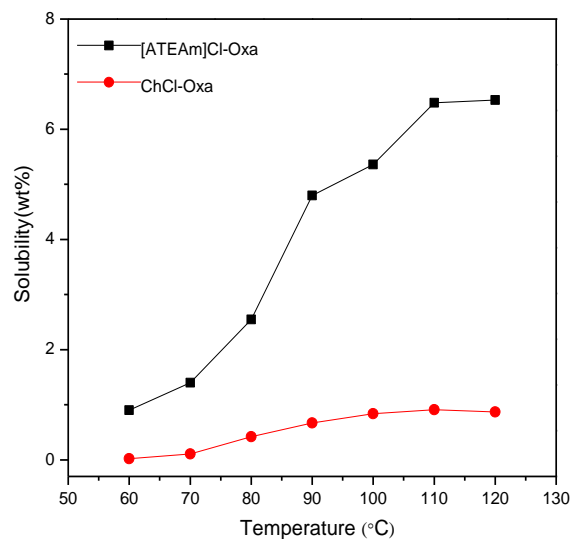
where  $\eta$  represents the value of viscosity,  $T$  is the absolute temperature,  $E_\eta$  is the pseudo activation energy for viscous flow, and  $\eta_0$  is a constant. The values of the parameters  $\eta_0$ ,  $E_\eta$ , and  $R^2$  are listed in Fig. 4. A good linear correlation was observed between  $\ln \eta$  and  $1/T$  values over the two DESs ( $R^2 > 0.97$ ). The [ATEAm]Cl-Oxa showed low  $E_\eta$  values (44.56 kJ mol<sup>-1</sup>) compared with ChCl-Oxa (57.82 kJ mol<sup>-1</sup>). The low  $E_\eta$  value suggested a weaker entanglement of hydrogen bonds between chloride and Oxa in [ATEAm]Cl-Oxa. The [ATEAm]Cl-Oxa may release more free active ions to react with the hydrogen bonds in cellulose to improve dissolution.

### Dissolving of Cellulose in Allyl-functionalized DES

The solubility of cellulose in the two DESs increased as the temperature was increased from 60 °C to 120 °C (Fig. 5). The highest solubility (6.48 wt.%) for [ATEAm]Cl-Oxa occurred at 110 °C. Higher temperatures (> 110 °C) may cause decomposition of [ATEAm]Cl-Oxa, thereby decreasing the dissolving ability (Wang *et al.* 2012; Vigier and Jérôme 2013). The [ATEAm]Cl-Oxa exhibited far higher solubility than ChCl-Oxa at the same temperature by allylic substitution.

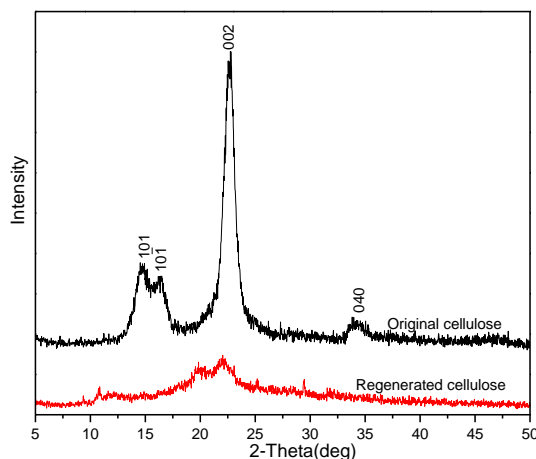


**Fig. 4.** Viscosity-temperature relationship of the DESs and Arrhenius fitted curves of  $\ln\eta$  versus  $1/T$  for the DESs. [ATEAm]Cl-Oxa:  $\eta_0 = 116.7$ ,  $E_\eta = 44.56$  kJ/mol,  $R^2 > 0.96$ ; ChCl-Oxa:  $\eta_0 = 113.29$ ,  $E_\eta = 57.82$  kJ/mol,  $R^2 > 0.99$ .



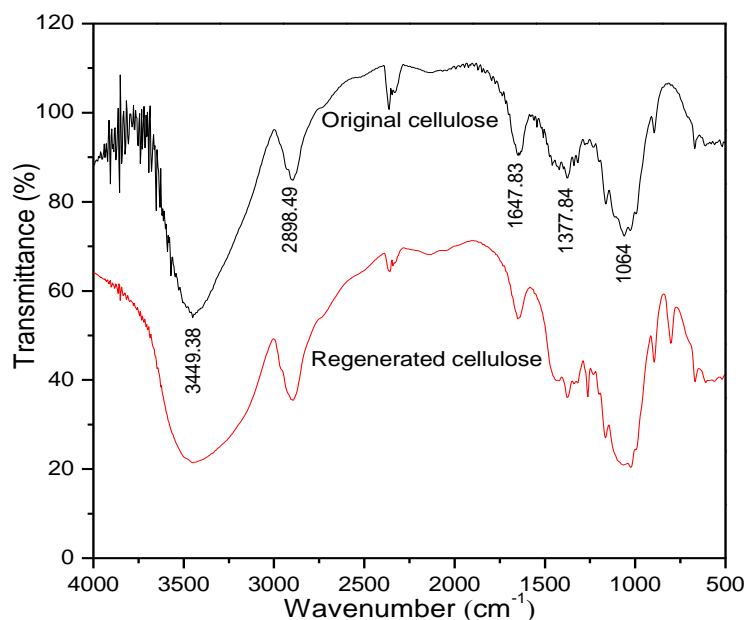
**Fig. 5.** Solubility of cellulose in [ATEAm]Cl-Oxa and ChCl-Oxa over temperature

The original cellulose showed characteristic diffraction curves of cellulose I (Fig. 6). The crystalline peaks at  $14.93^\circ$  ( $101$  plane),  $16.57^\circ$  ( $10\bar{1}$  plane), and  $22.84^\circ$  ( $002$  plane) were observed. The  $CrI$  of the original cellulose was 85.4%, which indicated that the crystalline structure dominated. The broader and weaker diffraction peaks appeared for the [ATEAm]Cl-Oxa dissolved cellulose. The shifted peaks ( $2\theta = 22.06$ ), reduced  $CrI$  (55.38%), and dropped peak intensity suggests the crystal form was changed from I to II. The results were consistent with the previous reports (Wang *et al.* 2015; Zhang *et al.* 2015).



**Fig. 6.** XRD patterns of original cellulose and regenerated cellulose from dissolving [ATEAm]Cl-Oxa

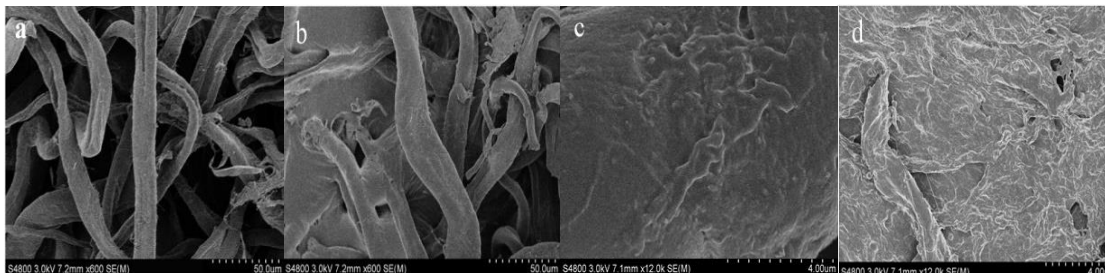
The FTIR characteristic peak at  $3449\text{ cm}^{-1}$  ( $-\text{OH}$  group) was unchanged after dissolution, which suggested that cellulose was directly dissolved in [ATEAm]Cl-Oxa and that no derivatives were generated (Fig. 7). The slight blue shifts, increased peak width, enhanced peak strength, and newly occurred small peaks in the fingerprint region of the regenerated cellulose all demonstrate the breaking of hydrogen bonds in cellulose, which was consistent with previous studies (Sirviö *et al.* 2015; Rashid *et al.* 2016). The fibrils of regenerated cellulose (Fig. 8b) became swollen compared to the original cellulose (Fig. 8a). The surface of the original cellulose was ordered and condensed under the SEM (Fig. 8c). The surface became rough and disordered after being dissolved by [ATEAm]Cl-Oxa (Fig. 8d). More accessible surface area would benefit the subsequent processing of regenerated cellulose (Singh *et al.* 2009).



**Fig. 7.** FTIR spectra of the original cellulose and regenerated cellulose from [ATEAm]Cl-Oxa dissolution

**Table 2.** Band Assignments in Original and Regenerated Cellulose for FTIR Spectra

Band of cellulose (cm <sup>-1</sup> )		Assignment
original	regenerated	
3449	3455	O–H vibrations
2898	2904	Strong C–H vibrations in saturated hydrocarbon groups
1647	1654	C=O stretching (Conjugated)
1377	1389	Strong C–H vibrations in saturated hydrocarbon groups
1064	1072	Strong C–O deformation in primary alcohol

**Fig. 8.** SEM micrographs of the original cellulose (a and c) and regenerated cellulose (b and d) from [ATEAm]Cl-Oxa dissolution

## CONCLUSIONS

1. A novel allyl-functionalized deep eutectic solvent (DES), the [ATEAm]Cl-Oxa, was synthesized based on allylic substitution of –OH group in choline cation.
2. The allyl group induced  $\pi$ - $\pi$  conjugative effect formed a charge-delocalized system on [ATEAm]<sup>+</sup>. Accordingly, the solvation properties and viscosity of [ATEAm]Cl-Oxa were improved and the solubility of cellulose was significantly promoted.
3. This study demonstrated a simple and effective functionalization method of DESs for superior dissolution of cellulose.

## ACKNOWLEDGMENTS

This work was supported by the National Natural Science Foundation of China (No. 20976107), the Science Foundation of China University of Petroleum, Beijing (2462014YJRC001), and the Research Fund for the Doctoral Program of Higher Education of China (20130007120007).

## REFERENCES CITED

- Abbott, A. P., Boothby, D., Capper, G., Davies, D. L., and Rasheed, R. K. (2004). “Deep eutectic solvents formed between choline chloride and carboxylic acids: Versatile alternatives to ionic liquids,” *J. Am. Chem. Soc.* 126(29), 9142-9147. DOI: 10.1021/ja048266j

- Abbott, A. P., Capper, G., Davies, D. L., Rasheed, R. K., and Tambyrajah, V. (2003). "Novel solvent properties of choline chloride/urea mixtures," *Chem. Commun.* (1), 70-71. DOI: 10.1039/B210714G
- Alvira, P., Tomas-Pejo, E., Ballesteros, M., and Negro, M. J. (2010). "Pretreatment technologies for an efficient bioethanol production process based on enzymatic hydrolysis: A review," *Bioresource Technol.* 101(13), 4851-4861. DOI: 10.1016/j.biortech.2009.11.093
- Badgajar, K. C., and Bhanage, B. M. (2015). "Factors governing dissolution process of lignocellulosic biomass in ionic liquid: Current status, overview and challenges," *Bioresource Technol.* 178, 2-18. DOI: 10.1016/j.biortech.2014.09.138
- Bergthaller, P. (1980). "Process for the polymerization of allyl ammonium salts and the resulting products," U.S. Patent No. 4329441.
- Boerstoel, H., Maatman, H., Westerink, J. B., and Koenders, B. M. (2001). "Liquid crystalline solutions of cellulose in phosphoric acid," *Polymer* 42(17), 7371-7379. DOI: 10.1016/S0032-3861(01)00210-5
- Castro, M. C., Arce, A., Soto, A., and Rodríguez, H. (2015). "Influence of methanol on the dissolution of lignocellulose biopolymers with the ionic liquid 1-ethyl-3-methylimidazolium acetate," *Ind. Eng. Chem. Res.* 54(39), 9605-9614. DOI: 10.1021/acs.iecr.5b02604
- Chowdhury, Z. Z., Hamid, S. B. A., Zain, S. M., and Khalid, K. (2014). "Catalytic role of ionic liquids for dissolution and degradation of biomacromolecules," *BioResources* 9(1), 1787-1823. DOI: 10.15376/biores.9.1.1787-1823
- Cruz, H., Fanselow, M., Holbrey, J. D., and Seddon, K. R. (2012). "Determining relative rates of cellulose dissolution in ionic liquids through *in situ* viscosity measurement," *Chem. Commun.* 48(45), 5620-5622. DOI: 10.1039/C2CC31487H
- Du, W., Liang, F., Jing, M., and Zhang, Y. (2013). "Synthesis and characterization of triethyl-allyl ammonia chloride," *Chemical Reagents* 35(11), 1045-1047, 1050.
- Francisco, M., Bruinhorst, A. V. D., and Kroon, M. C. (2012). "New natural and renewable low transition temperature mixtures (LTTMs): Screening as solvents for lignocellulosic biomass processing," *Green Chem.* 14(8), 2153-2157. DOI: 10.1039/C2GC35660K
- Francisco, M., González, A. S. B., Dios, S. L. G. D., Weggemans, W., and Kroon, M. C. (2013). "Comparison of a low transition temperature mixture (LTTM) formed by lactic acid and choline chloride with choline lactate ionic liquid and the choline chloride salt: Physical properties and vapour-liquid equilibria of mixtures containing water and ethanol," *RSC Adv.* 3, 23553-23561. DOI: 10.1039/C3RA40303C
- Garcia, H., Ferreira, R., Petkovic, M., Ferguson, J. L., Leitão, M. C., Gunaratne, H. Q. N., Seddon, K. R., Rebelo, L. P. N., and Pereira, C. S. (2010). "Dissolution of cork biopolymers in biocompatible ionic liquids," *Green Chem.* 12(3), 367-369. DOI: 10.1039/B922553F
- Gericke, M., Fardim, P., and Heinze, T. (2012). "Ionic liquids - promising but challenging solvents for homogeneous derivatization of cellulose," *Molecules* 17(6), 7458-7502. DOI: 10.3390/molecules17067458
- Gümüşkaya, E., Usta, M., and Kirci, H. (2002). "The effects of various pulping conditions on crystalline structure of cellulose in cotton linters," *Polym. Degrad. Stabil.* 81, 559-564. DOI: 10.1016/S0141-3910(03)00157-5

- Hou, X., Smith, T. J., Li, N., and Zong, M. (2012). "Novel renewable ionic liquids as highly effective solvents for pretreatment of rice straw biomass by selective removal of lignin," *Biotechnol. Bioeng.* 109(10), 2484-2493. DOI: 10.1002/bit.24522
- Huber, T., Müssig, J., Curnow, O., Pang, S., Bickerton, S., and Staiger, M. P. (2012). "A critical review of all-cellulose composites," *J. Mater. Sci.*, 47(3), 1171-1186. DOI: 10.1007/s10853-011-5774-3
- Isik, M., Gracia, R., Kollnus, L. C., Tomé, L. C., Marrucho, I. M., and Mecerreyes, D. (2013). "Cholinium-based poly(ionic liquid)s: Synthesis, characterization, and application as biocompatible ion gels and cellulose coatings," *ACS Macro Letters* 2(11), 975-979. DOI: 10.1021/mz400451g
- Itoh, T. (2014). "Design of ionic liquids for cellulose dissolution," in: *Production of Biofuels and Chemicals with Ionic Liquids*, Z. Fang, R. L. Smith, and X. Qi (eds.), Springer Science+Business Media B.V., Dordrecht, Netherlands, pp. 91-106.
- Juneidi, I., Hayyan, M., and Hashim, M. A. (2015). "Evaluation of toxicity and biodegradability for cholinium-based deep eutectic solvents," *RSC Adv.* 5(102), 83636-83647. DOI: 10.1039/C5RA12425E
- Kamlet, M. J., and Taft, R. W. (1976). "The solvatochromic comparison method. I. Beta-scale of solvent hydrogen-bond acceptor (HBA) basicities," *J. Am. Chem. Soc.* 98(2), 377-383. DOI: 10.1021/ja00418a009
- Kilpeläinen, I., Xie, H., King, A., Granstrom, M., Heikkinen, S., and Argyropoulos, D. S. (2007). "Dissolution of wood in ionic liquids," *J. Agric. Food Chem.* 55(22), 9142-9148. DOI: 10.1021/jf071692e
- Klemm, D., Heublein, B., Fink, H. P., and Bohn, A., (2005). "Cellulose: Fascinating biopolymer and sustainable raw material," *Angew. Chem. Int. Ed.* 44(22), 3358-3393. DOI: 10.1002/anie.200460587
- Nayak, J. N., Chen, Y., and Kim, J. (2008). "Removal of impurities from cellulose films after their regeneration from cellulose dissolved in DMAc/LiCl solvent system," *Ind. Eng. Chem. Res.* 47(5), 1702-1706. DOI: 10.1021/ie0710925
- Neumann, J., Steudte, S., Cho, C. W., Thöming, J., and Stolte, S. (2014). "Biodegradability of 27 pyrrolidinium, morpholinium, piperidinium, imidazolium and pyridinium ionic liquid cations under aerobic conditions," *Green Chem.* 16(4), 2174-2184. DOI: 10.1039/C3GC41997E
- Ohira, K., Abe, Y., Kawatsura, M., and Suzuki, K. (2012). "Design of cellulose dissolving ionic liquids inspired by nature," *ChemSusChem* 5(2), 388-391. DOI: 10.1002/cssc.201100427
- Paiva, A., Craveiro, R., Aroso, I., Martins, M., Reis, R. L., and Duarte, A. R. C. (2014). "Natural deep eutectic solvents – Solvents for the 21st century," *ACS Sustainable Chemistry & Engineering* 2(5), 1063-1071. DOI: 10.1021/sc500096j
- Pretti, C., Chiappe, C., Baldetti, I., Brunini, S., Monni, G., and Intorre, L. (2008). "Acute toxicity of ionic liquids for three freshwater organisms: *Pseudokirchneriella subcapitata*, *Daphnia magna* and *Danio rerio*," *Ecotoxicology and Environmental Safety* 72(4), 1170-1176. DOI: 10.1016/j.ecoenv.2008.09.010
- Ramamoorthy, S. K., Skrifvars, M., and Persson, A. (2015). "A review of natural fibers used in biocomposites: Plant, animal and regenerated cellulose fibers," *Polym. Rev.* 55(1), 107-162. DOI: 10.1080/15583724.2014.971124
- Rashid, T., Kait, C. F., Regupathi, I., and Murugesan, T. (2016). "Dissolution of kraft lignin using Protic Ionic Liquids and characterization," *Ind. Crops Prod.* 84, 284-293. DOI: 10.1039/c5gc00398a

- Ru, G., Luo, H., Liang, X., Wang, L., Liu, C., and Feng, J. (2015). "Quantitative NMR investigation on the low-temperature dissolution mechanism of chitin in NaOH/urea aqueous solution," *Cellulose* 22(4), 2221-2229. DOI: 10.1007/s10570-015-0667-2
- Saelee, K., Yingkamhaeng, N., Nimchua, T., and Sukyai, P. (2016). "An environmentally friendly xylanase-assisted pretreatment for cellulose nanofibrils isolation from sugarcane bagasse by high-pressure homogenization," *Ind. Crop. Prod.* 82, 149-160. DOI: 10.1016/j.indcrop.2015.11.064
- Sathitsuksanoh, N., George, A., and Zhang, Y. H. P. (2013). "New lignocellulose pretreatments using cellulose solvents: A review," *J. Chem. Technol. Biot.* 88(2), 169-180. DOI: 10.1002/jctb.3959
- Segal, L., Creely, J. J., Martin, A. E., and Conrad, C. M. (1959). "An empirical method for estimating the degree of crystallinity of native cellulose using the X-ray diffractometer," *Text. Res. J.* 29(10), 786-794. DOI: 10.1177/004051755902901003
- Singh, S., Simmons, B. A., and Vogel, K. P. (2009). "Visualization of biomass solubilization and cellulose regeneration during ionic liquid pretreatment of switchgrass," *Biotechnol. Bioeng.* 104(1), 68-75. DOI: 10.1002/bit.22386
- Sirviö, J. A., Visanko, M., and Liimatainen, H. (2015). "Deep eutectic solvent system based on choline chloride-urea as a pre-treatment for nanofibrillation of wood cellulose," *Green Chem.* 17, 3401-3406. DOI: 10.1039/c5gc00398a
- Spange, S., Fischer, K., Prause, S., and Heinze, T. (2003). "Empirical polarity parameters of celluloses and related materials," *Cellulose* 10(3), 201-212. DOI: 10.1023/A:1025197520736
- Sun, N., Rodríguez, H., Rahman, M., and Rogers, R. D. (2011). "Where are ionic liquid strategies most suited in the pursuit of chemicals and energy from lignocellulosic biomass?" *Chem. Commun.* 47(5), 1405-1421. DOI: 10.1039/C0CC03990J
- Taft, R. W., and Kamlet, M. J. (1976). "The solvatochromic comparison method. II. Alpha-scale of solvent hydrogen-bond donor (HBD) acidities," *J. Am. Chem. Soc.* 98(10), 2886-2894. DOI: 10.1021/ja00426a036
- Tang, B., and Row, K. H. (2013). "Recent developments in deep eutectic solvents in chemical sciences," *Monatshefte für Chemie* 144(10), 1427-1454. DOI: 10.1007/s00706-013-1050-3.
- Tang, S., Baker, G. A., Ravula, S., Jones, J. E., and Zhao, H. (2012). "PEG-functionalized ionic liquids for cellulose dissolution and saccharification," *Green Chem.* 14(10), 2922-2932. DOI: 10.1039/C2GC35631G
- Vigier, K. D. O., and Jérôme, F. (2013). "Choline chloride-derived ILs for activation and conversion of biomass," in: *Production of Biofuels and Chemicals with Ionic Liquids*, Z. Fang, R. L. Smith, and X. Qi (eds.), Springer Science+Business Media B.V., Dordrecht, Netherlands, pp. 61-87.
- Vitz, J., Erdmenger, T., Haensch, C., and Schubert, U. S. (2009). "Extended dissolution studies of cellulose in imidazolium based ionic liquids," *Green Chem.* 11(3), 417-424. DOI: 10.1039/B818061J
- Wang, G., Guo, J., Zhuang, L., Wang, Y., and Xu, B. (2015). "Dissolution and regeneration of hide powder/cellulose composite in Gemini imidazolium ionic liquid," *Int. J. Biol. Macromol.* 76, 70-79. DOI: 10.1016/j.ijbiomac.2015.02.029
- Wang, H., Gurau, G., and Rogers, R. D. (2012). "Ionic liquid processing of cellulose," *Chem. Soc. Rev.* 41(4), 1519-1537. DOI: 10.1039/C2CS15311D

- Xia, S., Baker, G. A., Li, H., Ravula, S., and Zhao, H. (2014). "Aqueous ionic liquids and deep eutectic solvents for cellulosic biomass pretreatment and saccharification," *RSC Adv.* 4(21), 10586-10596. DOI: 10.1039/C3RA46149A
- Zavrel, M., Bross, D., Funke, M., Büchs, J., and Spiess, A. C. (2009). "High-throughput screening for ionic liquids dissolving (ligno-)cellulose," *Bioresource Technol.* 100(9), 2580-2587. DOI: 10.1016/j.biortech.2008.11.052
- Zhang, H., Wu, J., Zhang, J., and He, J. (2005). "1-Allyl-3-methylimidazolium chloride room temperature ionic liquid: A new and powerful nonderivatizing solvent for cellulose," *Macromolecules* 38(20), 8272-8277. DOI: 10.1021/ma0505676
- Zhang, Q., Benoit, M., Vigier, K. D. O., Barrault, J., and Jérôme, F. (2012a). "Green and inexpensive choline-derived solvents for cellulose decrystallization," *Chem. Eur. J.* 18(4), 1043-1046. DOI: 10.1002/chem.201103271
- Zhang, Q., Vigier, K. D. O., Royer, S., and Jérôme, F. (2012b). "Deep eutectic solvents: Syntheses, properties and applications," *Chem. Soc. Rev.* 41(21), 7108-7146. DOI: 10.1039/C2CS35178A
- Zhang, T., Liu, X., Jiang, M., Duan, Y., and Zhang, J. (2015). "Effect of cellulose solubility on the thermal and mechanical properties of regenerated cellulose/graphene nanocomposites based on ionic liquid 1-allyl-3-methylimidazolium chloride," *RSC Adv.* 5(93), 76302-76308. DOI: 10.1039/C5RA15160K
- Zhao, Y., Liu, X., Wang, J., and Zhang, S. (2012). "Effects of cationic structure on cellulose dissolution in ionic liquids: A molecular dynamics study," *ChemPhysChem* 13(13), 3126-3133. DOI: 10.1002/cphc.201200286

Article submitted: June 5, 2016; Peer review completed: July 30, 2016; Revised version received and accepted: August 8, 2016; Published: August 23, 2016.  
DOI: 10.15376/biores.11.4.8457-8469